

# Blend Membranes Prepared from Cellulose and Soy Protein Isolate in NaOH/Thiourea Aqueous Solution

Yun Chen,<sup>1,2</sup> Lina Zhang<sup>1</sup>

<sup>1</sup>Department of Chemistry, Wuhan University, Wuhan 430072, China

<sup>2</sup>Research Center of Medicine and Structural Biology, Wuhan University, Wuhan 430072, China

Received 26 January 2004; accepted 14 May 2004

DOI 10.1002/app.20956

Published online in Wiley InterScience (www.interscience.wiley.com).

**ABSTRACT:** We have successfully prepared a series of blend membranes from cellulose and soy protein isolate (SPI) in NaOH/thiourea aqueous solution by coagulating with 5 wt % H<sub>2</sub>SO<sub>4</sub> aqueous solution. The structure and properties of the membranes were characterized by Fourier transform infrared spectroscopy, ultraviolet-visible spectrometry, dynamic mechanical thermal analysis, scanning electron microscopy (SEM), transmission electron microscopy, and tensile testing. The effects of SPI content ( $W_{\text{SPI}}$ ) on the structure and properties of the blend membranes were investigated. The results revealed that SPI and cellulose are miscible in a good or a certain extent when the SPI content is less than 40 wt %. The pore structure and properties of the blend membranes were significantly improved by incorporation of SPI into cellulose. With an increase in  $W_{\text{SPI}}$  from 10 to 50 wt %, the apparent size of the pore ( $2r_e$ ) measured by

SEM for the blend membranes increased from 115 nm to 2.43  $\mu\text{m}$ , and the pore size ( $2r_f$ ) measured by the flow rate method increased from 43 to 59 nm. The tensile strength ( $\sigma_b$ ) and thermal stability of the blend membranes with lower than 40 wt % of  $W_{\text{SPI}}$  are higher than that of the pure cellulose membrane, owing to the strong interaction between SPI and cellulose. The values of tensile strength and elongation at break for the blend membranes with 10 wt % of  $W_{\text{SPI}}$  reached 136 MPa and 12%, respectively. The blend membranes containing protein can be used in water because of keeping  $\sigma$  of 10 to 37 MPa. © 2004 Wiley Periodicals, Inc. *J Appl Polym Sci* 94: 748–757, 2004

**Key words:** blends; membranes; morphology; compatibility; mechanical properties

## INTRODUCTION

Sustainability, industrial ecology, ecoefficiency, and green chemistry are guiding the development of the next generation of materials, products, and processes.<sup>1</sup> Cellulose, an environmentally friendly material, is the most abundant natural polymer to yield various useful products because of its renewable, biodegradable, biocompatible, and derivable properties.<sup>2</sup> However, cellulose has not reached its potential applications, because it cannot be melted to fabricate into a desired form or to be dissolved in a common solvent, attributing to the strong intra- and intermolecular hydrogen bonding. Thus, more focus has been concentrated on new solvent systems of cellulose, including *N*-methylmorpholine-*N*-oxide (NMMO),<sup>3</sup> lithium chloride/*N*,*N*-dimethylacetamide (LiCl/DMAC),<sup>4–6</sup> and zinc chloride.<sup>7</sup> In our laboratory, novel solvents for cellulose have been developed, such as NaOH/urea<sup>8</sup> and NaOH/thiourea<sup>9</sup> aqueous solution. In these systems, addition of urea or thiourea to NaOH aqueous solution effectively destroys the intra- and intermolecular

hydrogen bonding and thus dissolves cellulose.<sup>10</sup> Moreover, cellulose/casein<sup>11</sup> and cellulose/alginate blend membranes<sup>12</sup> in NaOH/urea aqueous solution have been prepared, exhibiting a good tensile strength and relatively large pore size. It should be mentioned that the blended or regenerated cellulose and its derivative membranes have been widely applied in membrane separation technologies<sup>13,14</sup> and biological<sup>15</sup> and medical fields,<sup>16</sup> because of their chemical stability, biological compatibility, biodegradability, and high water ultrafiltration rate.

In recent years, soy products such as soy protein isolate (SPI), soy whole flour (SWF), and soy protein concentrated (SPC) have been considered as alternatives to petroleum polymers because of their abundant resources, low cost, perfect adhesivity, and good biodegradability.<sup>1,17</sup> Soy protein isolate was not only applied as an environmentally, friendly material in the fields of adhesives,<sup>18</sup> plastics,<sup>19,20</sup> and textile fibers,<sup>21</sup> but also as biodegradable membranes<sup>22</sup> or modified SPI films by sodium dodecyl sulfate.<sup>23</sup> Interestingly, SPI coated onto paper can enhance the grease resistance and mechanical properties,<sup>24</sup> suggesting that a certain interaction between SPI and cellulose occurs in this case. In our laboratory, the blend membranes prepared from cellulose with animal protein such as casein<sup>11</sup> and silk fibroin<sup>25,26</sup> in the new solvent sys-

Correspondence to: L. Zhang (Inzhang@public.wh.hb.cn).

**TABLE I**  
The Percentage of Weight Loss for the Membranes in Distilled Water and in 5 wt % NaOH Solution

Membrane no.	$W_{\text{SPI}}$ (%)	$W_{\text{loss}}$ (%)	
		In distilled water	In NaOH solution
CS1-0	0	0.23	0.58
CS1-10	10	0.65	9.37
CS1-20	20	1.03	17.95
CS1-30	30	1.55	27.42
CS1-40	40	1.98	36.67
CS1-50	50	3.71	43.54

tem<sup>8,9</sup> have some special porous properties and good mechanical properties, prompting potential applications in separation technology as well as biological and medical fields. In this work, we attempted to prepare a series of blend membranes from cellulose and SPI in NaOH/thiourea aqueous solution. The interaction between cellulose and SPI and the effects of SPI content on the structure and properties of the blend membranes throughout various characterizations were investigated and discussed.

## EXPERIMENTAL

### Materials

The cotton linter was supplied by Hubei Chemical Fiber Group Ltd. (Hubei, China), and its viscosity average molecular weight ( $M_v$ ) was determined by viscosimetry in cadoxen to be  $10.1 \times 10^4$ . Soy protein isolate was purchased from Hubei Yunmeng Protein Technology Co. (Hubei, China). The cotton linter and SPI were dried *in vacuo* for 24 h at 60°C before use. NaOH, thiourea, and  $\text{H}_2\text{SO}_4$  were analytical grade and were obtained from commercial resources in China.

### Preparation of membranes

Cotton linter was immersed in 6 wt % NaOH/5 wt % thiourea aqueous solution as described in detail elsewhere.<sup>27</sup> The mixture of cotton linter and 6 wt % NaOH/5 wt % thiourea aqueous solution was kept below  $-8^\circ\text{C}$  in a refrigerator for 12 h and then was taken out and thawed with stirring below 20°C for 1 h to obtain a cellulose solution. It was then centrifuged at 7,000 rpm for 30 min to give a transparent cellulose solution. The concentration of the cellulose solution was measured to be 3.7 wt % as the following. The weighted solution was poured into glacial acetic acid to form precipitation, which was isolated by filtration, washed with distilled water, and then dried *in vacuo* at 60°C for 24 h, and then weighted accurately again.<sup>28</sup> The concentration of cellulose was calculated from the weight ratio of the regenerated cellulose and the cellulose solution. SPI was dissolved in the 6 wt %

NaOH/5 wt % thiourea aqueous solution at room temperature to get a slurry with 10 wt % of SPI content. The SPI solution was mixed with the cellulose solution to obtain mixture solutions containing 10, 20, 30, 40, and 50 wt % of  $W_{\text{SPI}}$ , respectively. The resulting mixture solution was stirred at room temperature for 30 min and degassed at 10°C by centrifuging and then cast on a glass plate to provide a gel sheet with a thickness of about 200  $\mu\text{m}$ . It was immediately coagulated with 5 wt %  $\text{H}_2\text{SO}_4$  aqueous solution for 5 min to obtain transparent membranes. The obtained membranes were washed with water and then dried in air at room temperature, coded as CS1-*n* (cellulose/soy protein isolate blend), where *n* corresponds to the initially designed SPI content, for example, CS1-10 corresponds to 10 wt % of  $W_{\text{SPI}}$ . The membrane with more than 50 wt % of  $W_{\text{SPI}}$  was difficult to prepare with the procedure described above. As the control, the regenerated cellulose membrane without SPI thus was coded as CS1-0.

### Characterization

To investigate the interaction between cellulose and SPI, the weight loss of the membranes in distilled water was measured. The initial weight ( $W_0$ ) and the final weight ( $W_1$ ) were measured, respectively, before and after the membranes were immersed in distilled water at room temperature for 48 h. The membranes were dried *in vacuo* at 60°C for 24 h prior to each weighing. The percentage of weight loss ( $W_{\text{loss}}/\%$ ) for the membranes could be calculated by

$$W_{\text{loss}} = [(W_0 - W_1)/W_0] \times 100\% \quad (1)$$

The percentage of weight loss for the membranes in 5 wt % NaOH solution was measured according to the

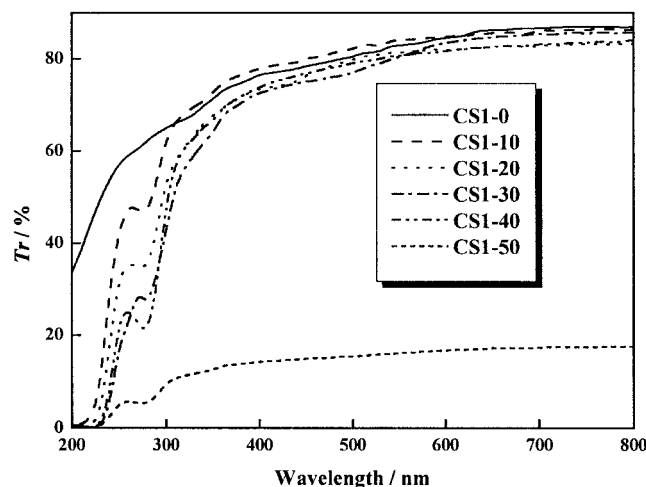


**Figure 1** The UV-Vis optical transmittance ( $Tr/\%$ ) curves of CS1-*n* membranes.

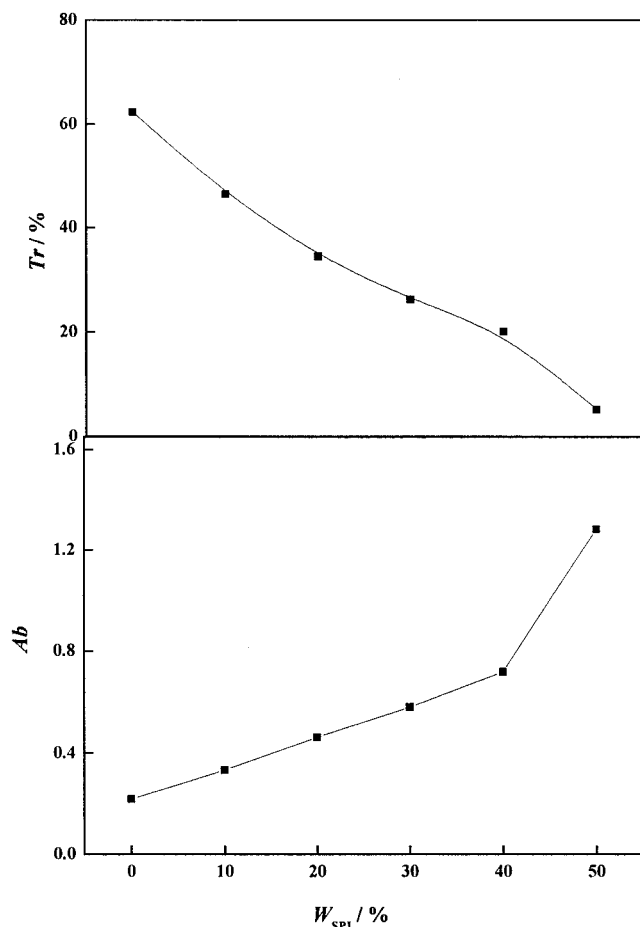


**Figure 2** The dependence of optical transmittance ( $Tr/\%$ ) and absorbency ( $Ab = -\log Tr$ ) of the CS1- $n$  membranes at 280 nm on  $W_{SPI}$ .

above process by replacing distilled water with 5 wt % NaOH solution. In this case, most of SPI was removed from the blend membranes, resulting in a weight loss.

The optical transmittance ( $Tr/\%$ ) of the membranes with a thickness of 20  $\mu\text{m}$  was measured using an ultraviolet-visible (UV-Vis) spectroscope (UV-160A, Shimadzu, Japan) in the wavelength range from 200 to 800 nm.

The membranes were dried *in vacuo* at room temperature for 24 h and cut into small pieces to be mixed with KBr for the disk before the measurements of Fourier transform infrared spectra (FT-IR). FT-IR spectra were recorded on an FT-IR spectrometer (1600, Perkin-Elmer Co., MA) in a wavenumber range from 4,000 to 400  $\text{cm}^{-1}$ .

The morphology was observed on a scanning electron microscope (SEM, S-570, Hitachi, Ibaraki, Japan), with 15 kV as the accelerating voltage, and recorded in a 35 mm film. The cellulose membrane and blend membranes were kept in water to maintain a wet state all through until they were sampled for SEM observation. The wet membranes were frozen in liquid nitro-

gen, fractured immediately, and freeze dried *in vacuo*, and then the free surfaces and cross-sections were coated with gold for SEM observation. The average apparent pore size ( $2r_c$ ) was measured from the SEM photographs of the surfaces and cross-sections by a high resolution imaging treatment system (HLPAS-1000, Tongji Medical College, Huazhong University of Science and Technology, Wuhan, China).

The ultrastructure of the blend membranes in the dry state was observed on a transmission electron microscope (TEM, H-600, Hitachi, Ibaraki, Japan), with 75 kV as the accelerating voltage, and recorded in a flat film. The membranes were stained by soaking in 1 wt %  $\text{OsO}_4$ , embedded in Epon-812 resin to harden and fix, and then cut into ultrathin sections with a

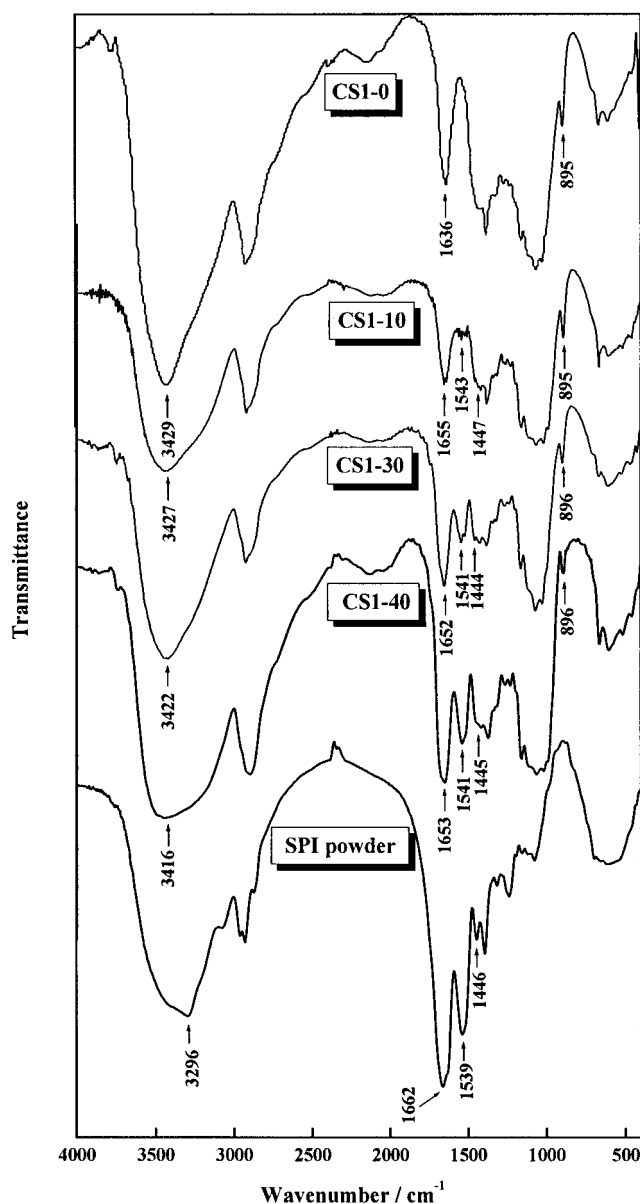


**Figure 3** FT-IR spectra of CS1- $n$  membranes and SPI powder.

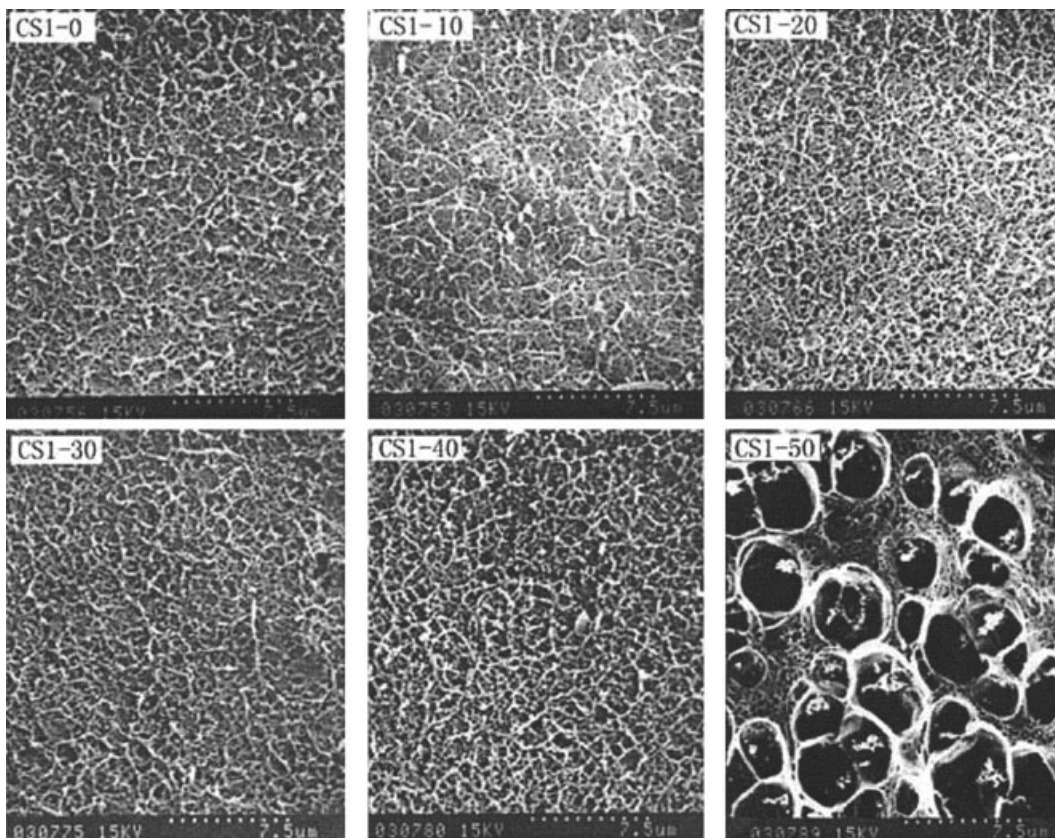


Figure 4 SEM photographs of the free surfaces for CS1-*n* membranes.

thickness of about 70 nm. The ultrathin sections were stained with plumb citrate for TEM observation.

An improved Bruss membrane osmometer based on the flow rate method, as reported by our laboratory,<sup>29</sup> was used for measuring the mean pore diameter ( $2r_f$ ) of the wet membranes. The values of  $2r_f$  were calculated by Kuhn's equation,<sup>30</sup> and membrane porosity ( $P_r$ ) was calculated according to the methods described previously elsewhere.<sup>29</sup>

$$2r_f = 2k\eta d(dv/dt)_i / (P_r \Delta P_i S) \quad (2)$$

$$k = 3.1 \times (1 - P_r^2)^{1/2} \quad (3)$$

$$P_r = 1 - W / (1.5\pi R^2 d) \quad (4)$$

where  $\eta$  is the absolute viscosity of fluid (alcohol) ( $\text{g s cm}^{-2}$ ),  $d$  is the thickness of the wet membrane (cm),  $(dv/dt)_i$  is the rate of the fluid flow through the membrane ( $\text{cm}^3 \text{s}^{-1}$ ),  $\Delta P_i$  is the pressure difference ( $\text{g cm}^{-2}$ ),  $S$  is the effective area of the membrane ( $\text{cm}^2$ ),  $P_r$  is the porosity,  $k$  is the apparent dimension of the pore distribution,  $W$  is the weight of the dry membrane (g), and  $R$  is the radius of the wet membrane (cm).

Dynamic mechanical thermal analysis (DMTA) was carried out on a dynamic mechanical thermal analyzer (DMTA-V, Rheometric Scientific Co., Amherst, MA) at

a frequency of 1 Hz. The specimens were heated at  $10^\circ\text{C min}^{-1}$  to  $110^\circ\text{C}$  to remove moisture and then cooled to  $-80^\circ\text{C}$  by liquid nitrogen. The DMTA test temperature ranged from  $-80$  to  $400^\circ\text{C}$  with a heating rate of  $5^\circ\text{C min}^{-1}$ .

The mechanical properties of the membranes were tested on a universal testing machine (CMT6503, Shenzhen SANS Test Machine Co. Ltd., Shenzhen, China) according to ISO6239-1986 (E) at a tensile rate of  $5 \text{ mm min}^{-1}$ . The mean values of the tensile strength ( $\sigma_b$ ) and the elongation at break ( $\epsilon_b$ ) were obtained from more than three specimens. The membranes were immersed into water at  $25^\circ\text{C}$  for 1 h, and then their mechanical properties in the wet state were measured in the same way as above.

## RESULTS AND DISCUSSION

### Interaction between cellulose and SPI

The percentage of weight loss for the membranes in distilled water and in 5 wt % NaOH solution are listed in Table I. Because of the extremely low solubility of cellulose in water, the slight weight loss mainly resulted from the water-soluble component of SPI. The low  $W_{\text{loss}}$  of the blend membranes implies that both SPI and cellulose coexist in the blend membranes hav-

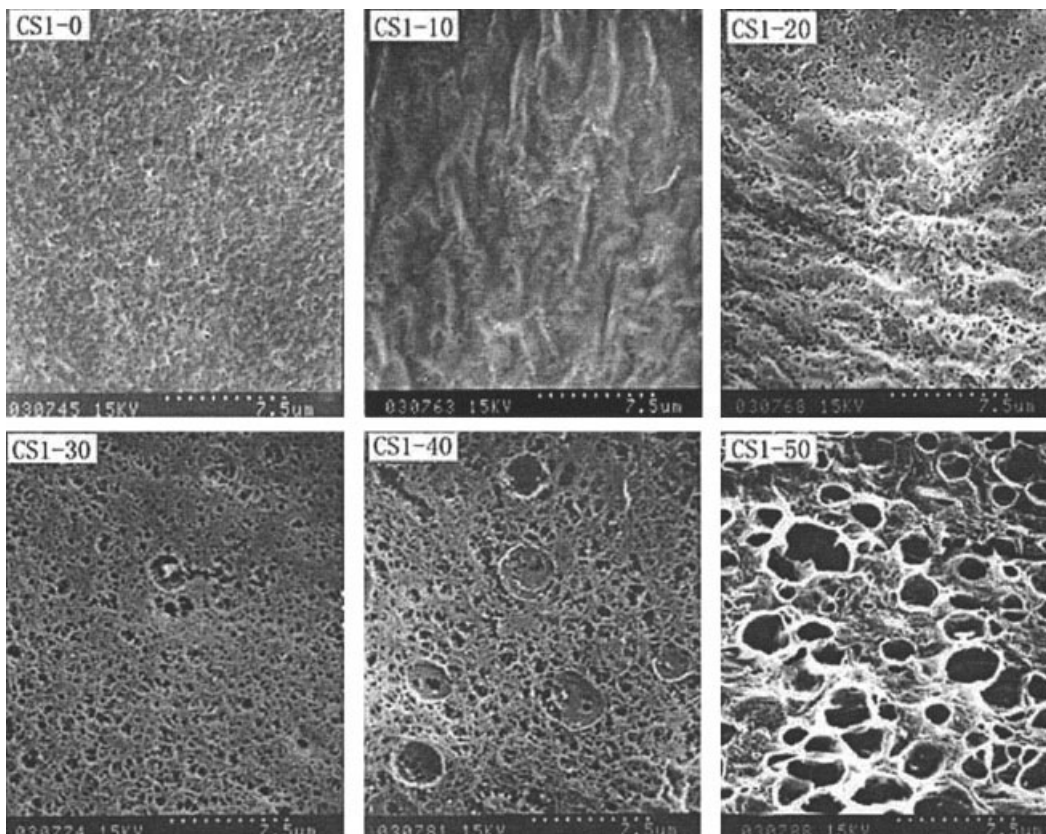


Figure 5 SEM photographs of the cross-sections for CS1-*n* membranes.

ing strong interaction caused by the hydrogen bonding between the hydroxyl groups of cellulose and amido groups of protein.<sup>14</sup> The percentage of weight loss for the membranes in 5 wt % NaOH solution was much larger than that in water, because most SPI can

be dissolved in NaOH solution, and a small amount of SPI combined tightly with cellulose still remained in the blend membranes.

The UV-Vis transmittance curves of the membranes are shown in Figure 1. The values of visible light

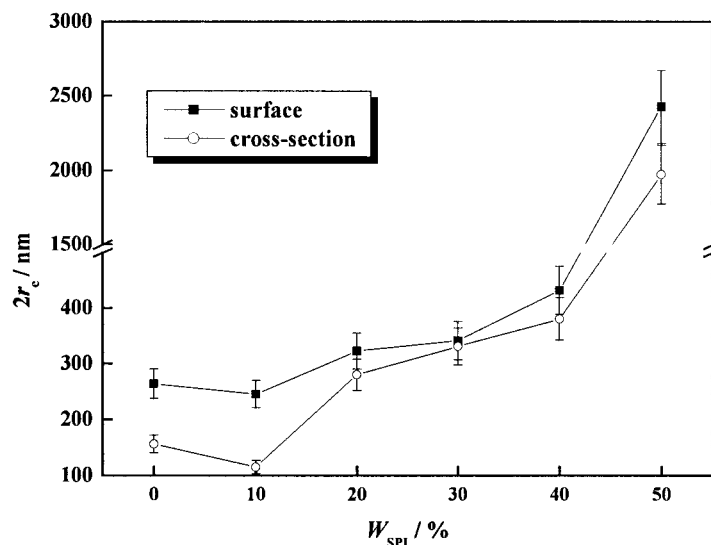


Figure 6 The dependence of apparent pore size ( $2r_c$ ) in the surfaces and cross-sections of CS1-*n* membranes on  $W_{\text{SPI}}$  measured by electron microscopy observation method.

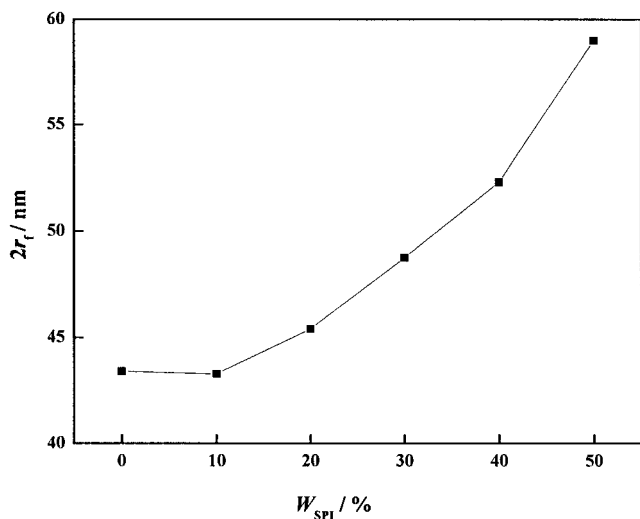


Figure 7 The dependence of mean pore size ( $2r_p$ ) of the membranes measured by the flow rate method on  $W_{SPI}$ .

transmittance (400 to 800 nm) for the blend membranes with 10 to 40 wt % of  $W_{SPI}$  and pure cellulose membranes are close to each other, and all are higher

than 70 %, indicating a high degree of compatibility between SPI and cellulose and of phase homogeneity in the blend membranes. However, the much lower  $Tr$  value of CS1-50 is a hint of a phase separation between cellulose and SPI. The  $Tr$  values of the membranes increase with an increase in wavelength. An obvious UV-resistivity in the wavelength range of 200 to 300 nm was exhibited. A reduction of transparency at 280 nm in all spectra is due to the absorption of protein at the wavelength.<sup>31</sup> The dependence of optical transmittance and absorbency ( $Ab$  equals  $-\log Tr$ ) of the CS1- $n$  membranes at 280 nm on  $W_{SPI}$  is shown in Figure 2. Obviously, the values of  $Ab$  at 280 nm rapidly and linearly increase with an increase in  $W_{SPI}$ . Invalidation of Beer's Law at 280 nm for CS1-50 indicates that the phase homogeneity no longer remains.

The IR spectra of CS1- $n$  are shown in Figure 3. The  $-\text{OH}$  stretching vibration bands around  $3,429 \text{ cm}^{-1}$  in cellulose membranes broadened and shifted to a lower wavenumber in the blend membranes, as a result of the introduction of protein composition into cellulose<sup>25</sup> and the formation of new hydrogen bonds.<sup>32</sup> As

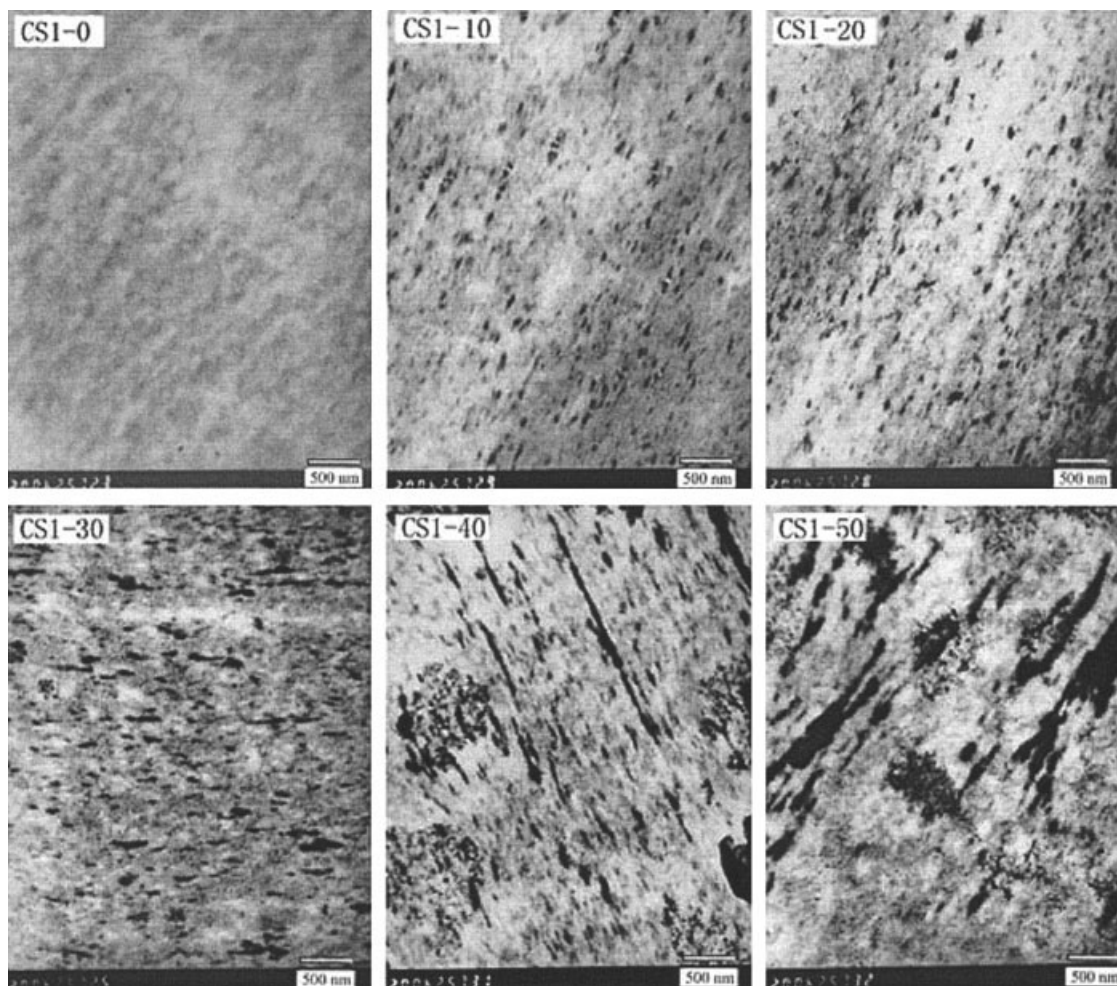


Figure 8 TEM photographs of CS1- $n$  membranes.

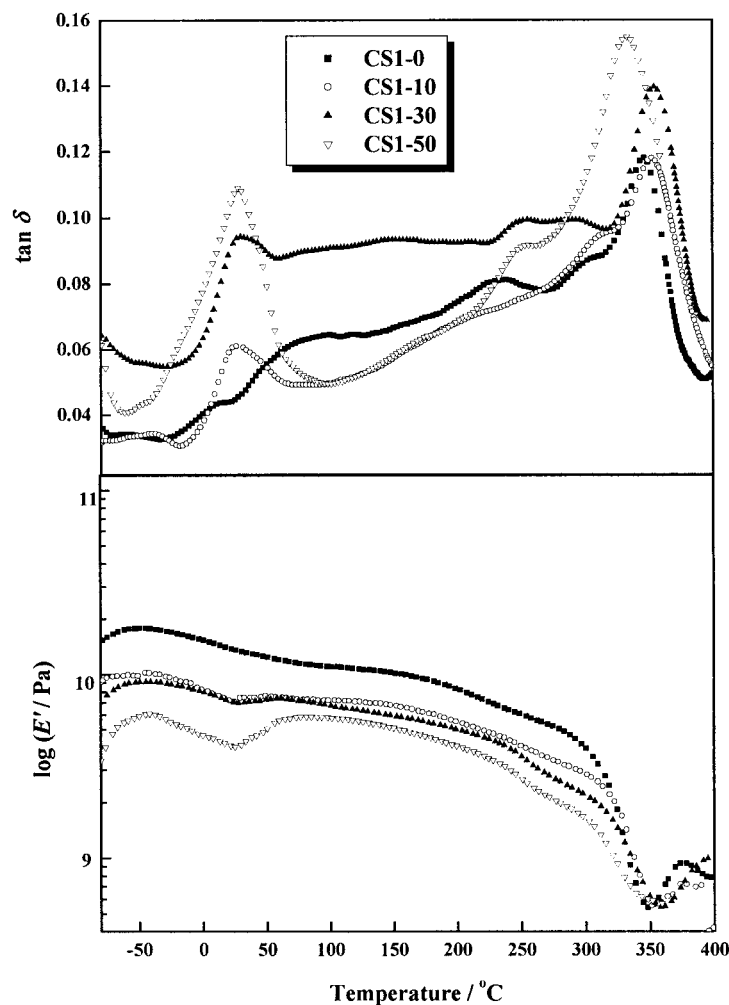


Figure 9 The dependence of  $\tan \delta$  and storage modulus ( $\text{Log } E'$ ) on temperature for CS1- $n$  membranes.

shown in Figure 3, cellulose and SPI exhibit carbonyl groups at  $1,636$  and  $1,662 \text{ cm}^{-1}$ , respectively. However, when they were blended, an apparent single absorption band (around  $1,653 \text{ cm}^{-1}$ ) appeared, indicating the presence of intermolecular hydrogen bonds between cellulose and protein molecules. In addition, with an increase in  $W_{\text{SPI}}$ , both the relative intensity at  $1,653$  and  $1,541 \text{ cm}^{-1}$  in the blend membranes increase, and the absorption peaks at about  $3,420 \text{ cm}^{-1}$  for the blend membranes broaden and shift to low wavenumbers, as a result of the intermolecular hydrogen bonds between cellulose and SPI.

#### Microstructure and pore size of the membranes

The SEM micrographs of CS1- $n$  membranes are shown in Figures 4 and 5. The  $W_{\text{SPI}}$  dependence of apparent pore size ( $2r_e$ ) calculated from SEM photographs of CS1- $n$  membranes is shown in Figure 6. These CS1- $n$  membranes display a homogenous mesh structure.<sup>12</sup> The apparent pore size is in a wide range from  $115 \text{ nm}$

to  $2.43 \mu\text{m}$ . The formation of the mesh structure in the surfaces and cross-sections for cellulose membrane is attributed to the self-aggregation tendency of cellulose in solution and the penetrating of coagulants in the coagulation process.<sup>33</sup> It can be explained that in the cellulose/NaOH/thiourea aqueous solution system, the presence of NaOH and thiourea can break the intermolecular hydrogen bonds of cellulose to create a significant ion–paris interaction, and the sodium ions, water, and thiourea molecules can form an “overcoat” surrounding the cellulose chains to prevent its self-aggregation, resulting in the significant increase of solubility of cellulose in the solvent system.<sup>34</sup> However, the addition of SPI broke off the “overcoat” surrounding the cellulose chains by a much stronger interaction between amido groups of SPI, and then the exposed hydroxyl groups of cellulose prompted the formation of a new physical crosslinking network with a bigger pore size than that of pure cellulose itself. The enormous number of hydrogen-bonding groups on the backbone of the two natural polymers is

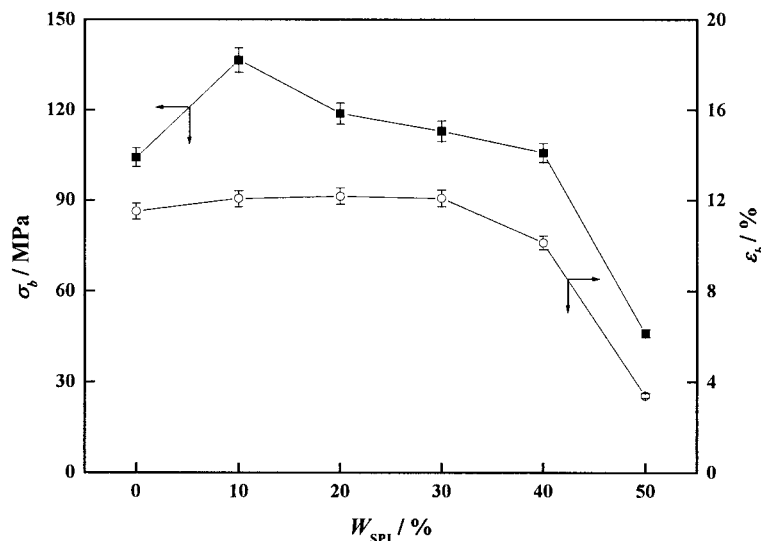


**Figure 10** The dependence of the tensile strength ( $\sigma_b$ ) and elongation at break ( $\epsilon_b$ ) in the dry state of CS1-*n* membranes on  $W_{SPI}$ .

the essential factor to their miscibility and stability in the blend membrane (*entropy effect*). As shown in Figures 4 to 6, the apparent pore size with the mesh structure woven by cellulose and SPI in the free surfaces and cross-sections of CS1-*n* increases with an increase of  $W_{SPI}$ . When  $W_{SPI}$  reaches 50 wt %, the  $2r_e$  of the surface and cross-section for CS1-50 are 2.43 and 1.97  $\mu\text{m}$ , respectively, which are much larger than those with lower  $W_{SPI}$ . Therefore, the membranes possess enough pore size in the surfaces, which could be used as an immobilized enzyme bioreactor<sup>15</sup> and as cell or organ support.<sup>16</sup> The pore size in the free surfaces and in the cross-sections for CS1-20 to CS1-40 are closed, indicating a relatively homogeneous pore structure exists in surfaces and in inner.

The dependence of the mean pore size ( $2r_f$ ) of the membranes measured by the flow rate method on  $W_{SPI}$  is shown in Figure 7. The  $2r_f$  values of the membranes increase with an increase in  $W_{SPI}$  except CS1-10. Both microscopic observation methods and the flow rate method are the main methods used to determine the pore size and its distribution in the porous membranes as reviewed by Zhao et al.<sup>35</sup> The values of  $2r_f$  are much smaller than those of  $2r_e$ . It is noted that the values of  $2r_f$  are related to only the interconnecting pores in the membranes during the filtration process.<sup>33</sup> However, those of  $2r_e$  include both the interconnecting and the much larger noninterconnecting (dead-end) pores.<sup>36</sup>

The visual proofs of a good miscibility between cellulose and SPI in our blend membranes are the TEM photographs as shown in Figure 8. The deep black regions are corresponding to the soy protein phase domains because protein is more easily stained than cellulose by plumb citrate, and the grayish re-

gions represent the cellulose phase. The size distribution of SPI phase domains is relatively uniform in the range from about 50 to 100 nm for the membranes CS1-10 to CS1-30. With an increase in  $W_{SPI}$ , the size of protein domain phases increase. The result of TEM indicates that soy protein coexists tightly with cellulose when  $W_{SPI}$  is lower than 40 wt %. In view of the results from UV-Vis, FT-IR, SEM, and TEM, good miscibility occurs between SPI and cellulose in blend membranes with lower than 40 wt % of  $W_{SPI}$ . The large pores of CS1-50 shown in Figures 4 and 5 were caused by the introduction of SPI, similar to the blend membranes from alginate and cellulose.<sup>12</sup>

The DMTA curves of the membranes are shown in Figure 9. The mechanical loss factor ( $\tan \delta$ ) reflects the mechanical relaxation behavior. The  $\tan \delta$  relaxation peaks at about 290 and 350°C are assigned to  $\alpha$  relaxation and decomposition temperature ( $T_d$ ) of the cellulose component, respectively.<sup>37</sup> The glass transition temperature ( $T_g$ ) of soy protein without plasticizers reported in literature is at about 145°C.<sup>38</sup> With an increase of plasticizers such as glycerol and water, the  $T_g$  appears at about -71 to about -35°C.<sup>39</sup> However, as shown in Figure 9, an obvious  $\tan \delta$  peak appears at 28–32°C in the blend membranes, and the height of the peak increases with an increase in  $W_{SPI}$ . The appearance of this peak must be related to SPI, because SPI chains were woven with cellulose to restrict molecular motion, leading to the strong interaction between SPI and cellulose. The  $\alpha$  relaxation and decomposition temperature of cellulose in the blend membranes, except in CS1-50, shifted to a higher temperature than that in the pure cellulose membrane, further confirming a strong interaction between cellu-



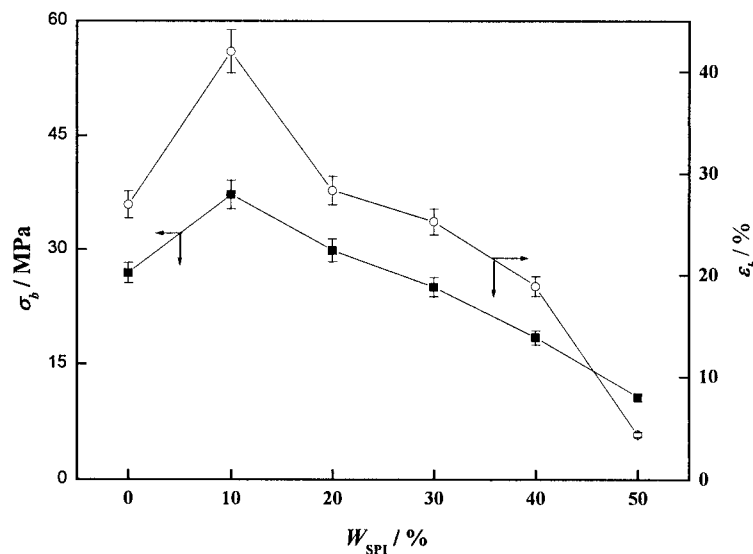


**Figure 11** The dependence of tensile strength ( $\sigma_b$ ) and elongation at break ( $\epsilon_b$ ) in the wet state of CS1-*n* membranes on  $W_{SPI}$ .

lose and SPI to enhance the thermal stability of the blend membranes.

### Mechanical properties

The dependences of  $\sigma_b$  and  $\epsilon_b$  values on  $W_{SPI}$  for CS1-*n* membranes in the dry and wet state are shown in Figures 10 and 11, respectively. The  $\sigma_b$  values of CS1-10 to CS1-40 and the  $\epsilon_b$  values of CS1-10 to CS1-30 membranes are higher than those of the pure regenerated cellulose membrane CS1-0. The  $\sigma_b$  and  $\epsilon_b$  values of CS1-10 membrane reach maxima: 136 MPa and 12%, respectively. The enhancement of the tensile strength of the blend membranes with  $W_{SPI}$  less than 40 wt % is another indicator for the strong interaction between cellulose and SPI. Although all the  $\sigma_b$  values of the membranes in the wet state are lower than those in the dry state, the blend membranes in the wet state still keep good tensile strength in a range from 10 to 37 MPa (except CS1-50), suggesting the membranes containing SPI can be used in water.

### CONCLUSION

New blend membranes of cellulose/SPI were prepared in 6 wt % of NaOH and 5 wt % of thiourea aqueous solution by coagulating with 5 wt %  $\text{H}_2\text{SO}_4$  solution. The blend membranes exhibited a mesh structure woven with cellulose and protein chains. With an increase in  $W_{SPI}$ , the apparent pore size in surfaces and cross-sections of the blend membranes measured by SEM and by the following rate method increased. The results from UV-Vis, FT-IR, SEM, TEM, and DMTA revealed good miscibility between cellulose and SPI in the blend membranes with less than 40 wt % of  $W_{SPI}$ , as a result of the strong hydrogen

bonding between hydroxyl groups of cellulose and amido groups of SPI molecules. Therefore, the introduction of SPI in the cellulose membranes enhanced the pore size and improved tensile strength and thermal stability of the blend membranes. The values of  $\sigma_b$ ,  $\epsilon_b$ , and  $T_d$  of the blend membranes containing less than 40 wt % of  $W_{SPI}$  in the dry state were higher than those of the pure cellulose membranes, and their  $\sigma_b$  values in the wet state still remain in the range from 10 to 37 MPa. This work provided the blend membranes from SPI and cellulose, which can be used in both dry and wet states.

The authors thank the National Natural Science Foundation of China for major grant 59933070 and the Key Laboratory of Cellulose Chemistry, Guangzhou Institute of Chemistry, Chinese Academy of Sciences.

### References

- Mohanty, A. K.; Misra, M.; Drzal, L. T. *J Polym Environ* 2002, 10, 19.
- Schurz, J. *Prog Polym Sci* 1999, 24, 481.
- Abe Y.; Mochizuki, A. *J Appl Polym Sci* 2002, 84, 2302.
- McCormick, C. L. US Patent No. 4278790, 1981.
- Dawsey, T. R.; McCormick, C. L. *J Macrol Sci Rev Macromol Chem Phys* 1990, C30, 405.
- Dupond, A. *Polymer* 2003, 44, 4117.
- Xu, Q.; Chen, L. F. *J Appl Polym Sci* 1999, 71, 1441.
- Zhou, J.; Zhang, L. *Polym J* 2000, 32, 866.
- Zhang, L.; Ruan, D.; Gao, S. *J Polym Sci Part B: Polym Phys* 2002, 40, 1521.
- Laszkiewicz, B.; Wcislo, P. *J Appl Poly Sci* 1990, 39, 415.
- Yang, G.; Zhang, L.; Han, H. *J Appl Polym Sci* 2001, 81, 3260.
- Zhou, J.; Zhang, L. *J Polym Sci Part B: Polym Phys* 2001, 39, 451.
- Gubitz, G.; Schmid, M. G. *Biopharm Drug Dispos* 2001, 22, 291.
- Zhang, L.; Yang, G.; Xiao, L. *J Membr Sci* 103, 1995, 65.
- Butterfield, D. A.; Bhattacharyya, D.; Daunert, S.; Bachas, L. *J Membr Sci* 2001, 181, 29.

16. Bartolo, L. D.; Morelli, S.; Bader, A.; Drioli, E. *Biomaterials* 2002, 23, 2485.
17. Paetau, I.; Chen, C.; Jane, J. *Ind Eng Chem Res* 1994, 33, 1821.
18. Hettiarachchy, N. S.; Kalapathy, U.; Myers, D. J. *J Am Oil Chem Soc* 1995, 72, 1461.
19. Zhang, J.; Mungara, P.; Jane, J. *Polymer* 2001, 42, 2569.
20. Chen, Y.; Zhang, L.; Du, L. *J Appl Poly Sci* 2003, 90, 3790.
21. Huang, H. C.; Hammond, E. G.; Reitmeier, C. A.; Myers, D. J. *J Am Oil Chem Soc* 1995, 72, 1453.
22. Brandenburg, A. H.; Weller, C. L.; Testin, R. F. *J Food Sci* 1993, 58, 1086.
23. Rhim, J. W.; Gennadios, A.; Weller, C. L.; Hanna, M. A. *Ind Crops Prod* 2002, 15, 99.
24. Park, H. J.; Kim, S. H.; Lim, S. T.; Shin, D. H.; Choi, S. Y.; Hwang, K. T. *J Am Oil Chem Soc* 2000, 77, 269.
25. Yang, G.; Zhang, L.; Liu, Y. *J Membr Sci* 2000, 177, 153.
26. Yang, G.; Zhang, L.; Cao, X.; Liu, Y. *J Membr Sci* 2002, 210, 379.
27. Zhang, L.; Ruan, D.; Gao, S. China Patent No. ZL 0012448.5, 2003.
28. Isogal, A.; Atalla, R. H. *Cellulose* 1998, 5, 309.
29. Yang, G.; Zhang, L. *J Membr Sci* 1996, 114, 149.
30. Kuhn, W.; Grenze, Z. *Z Electrochem Ber Bunsenges Physik Chem* 1951, 55, 207.
31. Roegerer, J.; Lutter, P.; Bluggel, M.; Meyer, T. E.; Anselmetti, D. *Anal Chem* 2003, 75, 157.
32. Kondo, T.; Sawatari, C.; Manley, R. S. J.; Gray, D. G. *Macromolecules* 1994, 27, 210.
33. Zhou, J.; Zhang, L.; Cai, J.; Shu, H. *J Membr Sci* 2002, 210, 77.
34. Weng, L.; Zhang, L.; Ruan, D.; Shi, L.; Xu, J. *Langmuir* 2004, 20, 2086.
35. Zhao, C.; Zhou, X.; Yue, Y. *Desalination* 2000, 129, 107.
36. Chen, Y.; Xiong, X.; Yang, G.; Zhang, L.; Lei, S.; Liang, H. *Chin J Polym Sci* 2002, 20, 369.
37. Yang, G.; Zhang, L.; Yamane, C.; Miyamoto, I.; Inamoto, M.; Okajima, K. *J Membr Sci* 1998, 139, 47.
38. Sue, H. J.; Wang, S.; Jane, J. *Polymer* 1997, 38, 5035.
39. Zhang, J.; Mungara, P.; Jane, J. *Polym Prepr* 1998, 39, 162.